OAK RIDGE
NATIONAL LABORATORY
MANAGED BY UT-BATTELLE
FOR THE DEPARTMENT OF ENERGY

ORNL/TM-2006/539

Evaluation of Cavitation-Erosion Resistance of 316LN Stainless Steel in Mercury Containing Metallic Solutes

August 2006

S. J. Pawel and L. K. Mansur

UT-BATTELLE

ORNL/TM-2006/539

Materials Science and Technology Division

Evaluation of Cavitation-Erosion Resistance of 316LN Stainless Steel in Mercury Containing Metallic Solutes

S. J. Pawel and L. K. Mansur

Date Published: August 2006

Prepared for the
U.S. Department of Energy
Spallation Neutron Source

Prepared by
OAK RIDGE NATIONAL LABORATORY
Oak Ridge, Tennessee 37831-6285
Operated by
UT-Battelle, LLC
for the
U. S. DEPARTMENT OF ENERGY
Under contract DE-AC05-00OR22725

CONTENTS

LIST OF TABLES

FIGURES

ABSTRACT

Room temperature cavitation tests of vacuum annealed type 316LN stainless steel were performed in pure mercury and in mercury with various amounts of metallic solute to evaluate potential mitigation of erosion/wastage. Tests were performed using an ultrasonic vibratory horn with specimens attached at the tip. All of the solutes examined, which included 5 wt % In, 10 wt % In, 4.4 wt % Cd, 2 wt % Ga, and a mixture that included 1 wt % each of Pb, Sn, and Zn, were found to increase cavitation-erosion as measured by increased weight loss and/or surface profile development compared to exposures for the same conditions in pure mercury. Qualitatively, each solute appeared to increase the tenacity of the post-test wetting of the mercury solutions and render the mercury mixture susceptible to manipulation of droplet shape.

1. INTRODUCTION

The Spallation Neutron Source (SNS) generates neutrons via interaction of a pulsed (60 Hz) 1.0 GeV proton beam with a liquid mercury target. The high energy pulses are expected to give rise to thermal-shock induced pressure waves in the mercury which, after reflection from the container surfaces, will result in negative pressure transients and cavitation in the target liquid.[1,2] Some of the energy released during the collapse of the cavitation bubbles near the containment surface will be manifested in a jetting action of liquid at extreme velocity that can potentially erode the containment material.

Based on a favorable combination of factors, including resistance to corrosion by mercury, well-characterized behavior in a neutron radiation environment, and retention of acceptable ductility after irradiation to moderate displacement doses, 316LN stainless steel was selected as the target container material.[3] However, previous tests have indicated that annealed 316LN is susceptible to potentially significant pitting and erosion damage resulting from cavitation in mercury using a split Hopkinson pressure bar (SHPB) apparatus,[4] in-beam exposures,[5,6] and a vibratory horn.[7–11] Of particular concern is the observation that pit depths resulting from relatively brief SHPB and in-beam exposures (order of 10–200 cavitation pulses/events), if linearly extrapolated over the anticipated target service life of several hundred million pulses, would prematurely threaten the integrity of the target containment.

It has been shown that the cavitation-erosion resistance of annealed 316LN may be improved by hardening the material via surface treatments and/or cold-working.[10,11] Further, cavitation-erosion resistance of alternate materials may be somewhat superior to 316LN,[10] but these alternate materials may exhibit less desirable or less well known properties for other aspects of the target service requirements.

It has also been observed that dissolving a significant amount of metallic elements into mercury leads to changes in surface tension characteristics of the liquid. In one particular experiment,[12] it was observed that a 4 wt % addition of alloying elements (primarily 1% each of Pb, Sn, and Zn along with smaller amounts of other elements) increased the surface tension about 35% compared to pure mercury. Further, droplets of the modified mercury formed at the end of a capillary tube were observed to become much larger and to stretch longer prior to breaking compared to the pure mercury counterparts, and the authors suggested the alloyed liquid appeared to be on the path to semi-solid behavior. If this would be the case, cavitation behavior in highly alloyed mercury might be expected to be significantly different than that in pure mercury,

particularly if the apparently semi-solid behavior of the alloyed mercury caused cavitation bubbles to collapse at lower velocities, thereby imparting less potential erosion damage on nearby containment surfaces.

In contrast to previous work,[10,11] which examined cavitation-erosion in mercury as a function of the physical properties of potential containment materials and various surface treatments, the concept under investigation here considers mercury composition as a potential variable to mitigate cavitation-erosion damage in a given structural material. While there are no doubt practical issues associated with alteration of the composition and fluid properties of the target mercury (such as pumping characteristics, neutron performance, and isotope generation/waste handling), the purpose of this laboratory effort was to compare cavitation damage on 316LN produced by pure mercury with that produced by mercury with various alloying additions.

2. EXPERIMENTAL

Binary phase diagrams[13] for mercury in combination with all other elements for which data were available were examined in the search for readily soluble alloying additions to mercury. Diagrams were located for mercury in combination with 74 different elements (although a few of the diagrams were calculated rather than observed/measured). Among these 74 elements, ambient temperature solubility in mercury was essentially nil for a large number of them and at least 1 wt % for only eleven elements. Of these eleven, three were dropped from further consideration in these screening tests due to handling dangers – primarily the potential for explosive oxidation – in the pure state (Cs, Rb, and Tl). Of the remaining eight soluble elements, Bi and Mg were deleted from the list of potential solutes because lab experiments suggested they oxidized too readily and presented very sluggish dissolution kinetics. The remaining six elements appear in Table 1 along with other information about each potential solute. The "mass discriminator" included in Table 1 simply relates the atomic mass of the potential solute to the atomic mass of mercury.

Table 1. Potential solutes for mercury in cavitation-erosion testing.

Element	Ambient solubility in mercury (wt%)[13]	Relative dissolution kinetics*	Relative mass**
Zn	~1	sluggish	0.33
Ga	~2	rapid	0.35
Cd	~5	rapid	0.56
In	~52	very rapid	0.57
Sn	~1	slow	0.59
Pb	~1	slow	1.03

*=$T \leq 30^{\circ}C$ modest agitation, argon cover gas
** = atomic mass of soluble element/atomic mass of mercury

During the initial experiments to assess solubility and dissolution kinetics, it was observed that in all cases for which some solubility was apparent, there was also simultaneous "creaming" of the surface of the mercury pool when the solution was prepared with exposure to air. The term "creaming" as used here describes the concept[12,14] that metals dissolved in mercury tend to have an extremely high activity in the atomic state and are therefore relatively reactive with even trace oxygen in the

environment. As a result, oxides of the solute metal tend to form quickly as a scum on the surface of the host mercury, and these oxides may also catalyze the oxidation of mercury itself. This effect is very readily apparent visually, as nominally clean/pure mercury has a very shiny silver surface whereas a “creamed” surface exhibits a dull gray layer that appears to encase the mercury. Although no attempt to quantify the relative amount or kinetics of scum formation was performed, it is clear that for solutes with a relatively high solubility, only a small fraction of the solute participates in scum formation even after a few days of contact with air. That this is so was evidenced qualitatively by attempts to filter the creamed mercury with cheesecloth, on which only a tiny mass compared to the mass of added solute was trapped. Similarly, a small amount of residual scum tends to remain behind in/on both glass and plastic bottles containing the mercury mixtures, but no residual film is left in/on either type of bottle while handling and pouring pure mercury. It may also be true that the scum is somewhat self-limiting in that its formation slows or precludes further reaction with air unless regularly disturbed (e.g., by stirring). In the absence of air (for example, under protective atmosphere or in evacuated chambers), the “creaming” reaction is drastically retarded and perhaps even eliminated on a practical time scale.

As a result of the tendency of the compositionally-modified mercury to reject solute at unknown and perhaps variable rates, it was determined that the vessel for the vibratory horn testing would require a mechanism to provide at least a modest inert cover gas to reduce the rate of solute reaction as much as practically possible. For mixtures utilizing elements relatively soluble in mercury, the loss of a small fraction of the total solute to the “creaming” reaction probably has only a small, if any, effect on cavitation test results, particularly over the short time period (typically two days) needed to perform a limited series of tests with a particular solution. However, for elements soluble in mercury to only about 1%, oxidation might be expected to consume sufficient solute during the test period to influence the solution properties and thereby the results.

In addition to the cover gas requirement, a test vessel with a relatively small volume of mercury was deemed useful in order to limit the total amount of solute necessary to make the test solutions. For example, previous cavitation tests in this laboratory utilized pure mercury in a ~750 ml bath contained within a wide-mouth stainless steel dewar. For such a large mercury volume, 5 wt % of a solute would correspond to more than 500 grams of relatively expensive metal (at least in the case of pure In, Cd, and Ga among the potential solutes considered). This was considered prohibitively expensive for these screening tests, so a glass vessel with a much smaller

volume (maximum of 100 ml) was fabricated for these experiments. Due to the limited volume of mercury in the test vessel, specimens were immersed only to a depth of approximately 2 mm for the test exposures unless otherwise noted.

Because of the intense energy/work associated with a vibratory horn cavitation test, the solution test temperature tends to increase during sonication. To maintain a constant temperature of the mercury bath during testing, the glass container was fabricated with a double wall to permit circulation of coolant around the mercury bath. It was found that setting the coolant temperature at ~15°C enabled a steady-state mercury temperature of 30-31°C during the cavitation test. Taking into consideration the need for an inert gas cover, reduced volume, and cooling capability, the vessel and test arrangement schematically depicted in Fig. 1 was used for all the tests presented here.

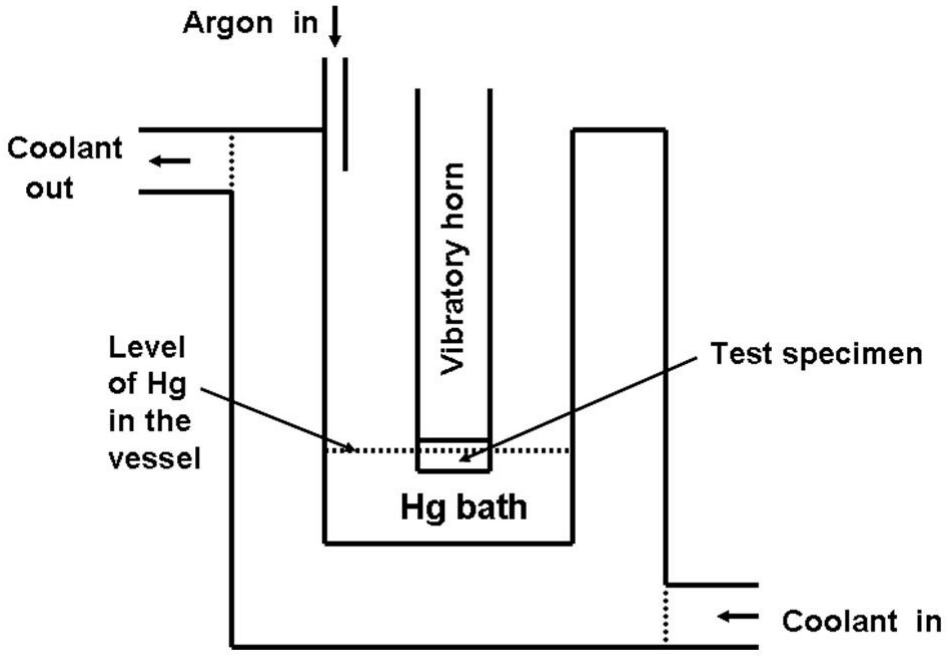

Fig. 1. Schematic drawing of the glass vessel used to contain the mercury in the present experiments. The specimen is on the tip of the vibratory horn submerged less than its full height (about 2 mm) into the mercury bath. Actual dimensions include an internal vessel diameter of 5 cm and a 1 cm gap between the bottom of the mercury containment and the test specimen surface.

All cavitation-erosion tests were performed using a titanium vibratory horn and the general test methodology described in ASTM G-32.[15] The working face of each test specimen had a surface area of 180 mm^2, and the specimen was attached to the vibratory horn via a threaded shank. Photos of the vibratory horn and representative specimens are given in Ref. 10. The horn tip oscillated at a fixed frequency (20 kHz) and was set to generate a peak-to-peak vibrational amplitude of approximately 25 μm. The rapid reciprocating displacement induces the formation and collapse of cavities in the liquid near the specimen surface, and cavitation-erosion damage from collapsing cavities can be quantified by measurement of specimen weight change and/or erosion depth as a function of exposure time. The baseline test condition included immersion of the working surface of the specimen to a depth of about 2 mm in approximately 30 ml of mercury, and a mercury test temperature maintained at approximately 30°C. For comparison, a small number of tests included an immersion depth of 25 mm in a somewhat larger amount of mercury (100 ml).

Nominally pure mercury (filtered through cheesecloth until the luster associated with the mercury surface was very bright/shiny) was used for baseline testing. Solutes examined in this set of screening tests included pure mercury with 5 wt % In, 10 wt % In, 4.4 wt % Cd, 2% Ga, and a mixture (following the example in Ref. 12) that included 1 wt % each of Zn, Pb, and Sn. To prepare the mixtures, the appropriate mass of solute in solid form was added to 30 ml of mercury in the glass test vessel with the cover gas already flowing (about 1 liter/min argon in a total vessel volume of about 0.25 liter, with the vessel open to room air around a loose-fitting lid or the neck of the vibratory horn). In the case of In (minutes at room temperature) and Cd and Ga (each an hour or so at 30°C), the solutions formed rapidly and testing commenced immediately with only minimal disruption of the cover gas to change test specimens. In the case of the mixture including Zn, Pb, and Sn, the solution was heated to 30°C and held under cover gas overnight, with occasional stirring, to establish the solution.

The test specimens were machined from a block of 316LN stainless steel that was also used as a source for specimens in previous testing.[10,11] The composition of the 316LN is given in Table 2. All specimens were machined from the original cross-rolled plate material such that the few inclusions present were oriented parallel to the test face. Following machining and light sanding of the test surface on 800 grit paper, the specimens were loosely wrapped in Ta-foil and vacuum annealed at 1020°C at 10^{-4} Pa (10^{-6} torr) or less for 1 h, followed by cooling to less than 300°C in about 1 h.

Table 2. Composition of master heat of 316LN stainless steel from certified mill report.

Element	Wt%	Element	Wt%
C	0.009	Cr	16.31
Mn	1.75	Ni	10.20
P	0.029	Mo	2.07
S	0.002	Co	0.16
Si	0.39	Cu	0.23
N	0.11	Fe	balance

Post-exposure cleaning of the specimens consisted of ultrasonic cleaning sequentially in (1) an aqueous solution containing dissolved sulfur species to chemically bind mercury, (2) distilled water, and (3) acetone, followed by forced air drying. Specimens were then weighed and examined with an optical microscope to determine the average cavitation-erosion profile and assess potential pitting.

The profile determination was performed with the calibrated fine focus feature of an optical microscope. Each division on the fine focus knob represents a one-micron vertical movement of the microscope stage, so by sequentially focusing first on the relative high point and then on the low point within a field of view, the depth of surface relief can be estimated. It should be noted that the surface profile measurement includes a modest subjectivity on the part of the observer, as a determination of the precise position (relative focus) of the high and low points in a field of view is relatively reproducible for a given observer but perhaps less so among different observers. In this experiment, the average profile was determined from measurements on seven random but regularly spaced fields of view at 400X, with observations of areas with surface profile significantly different than the average noted as appropriate. In addition, selected specimens were also examined with the scanning electron microscope.

3. RESULTS AND DISCUSSION

3.1 Data Interpretation

The evaluation reported here is intended primarily to compare cavitation-erosion damage among identical specimens in pure mercury and in modified mercury for a fixed test configuration. As such, it is a screening test only. In particular, the reader should recognize there is no precise correlation between the damage rate/intensity produced at the tip of the vibratory horn and at the surface of the mercury target container at the SNS target facility. Other details of data interpretation – generally less significant to the present investigation – appear in Refs. 10 and 11.

3.2 Baseline Testing – Pure Mercury

A series of three 1-h exposures was performed on four identically prepared specimens of vacuum annealed 316LN stainless steel in pure mercury. In each case, the mercury temperature was maintained at 30°C for specimens immersed to a depth of approximately 2 mm (about half the specimen thickness) into the mercury within the glass vessel previously described. These conditions will hereafter be referred to as the baseline test conditions to which other results will be compared. The weight loss results for annealed 316LN in the baseline test conditions are shown in Fig. 2.

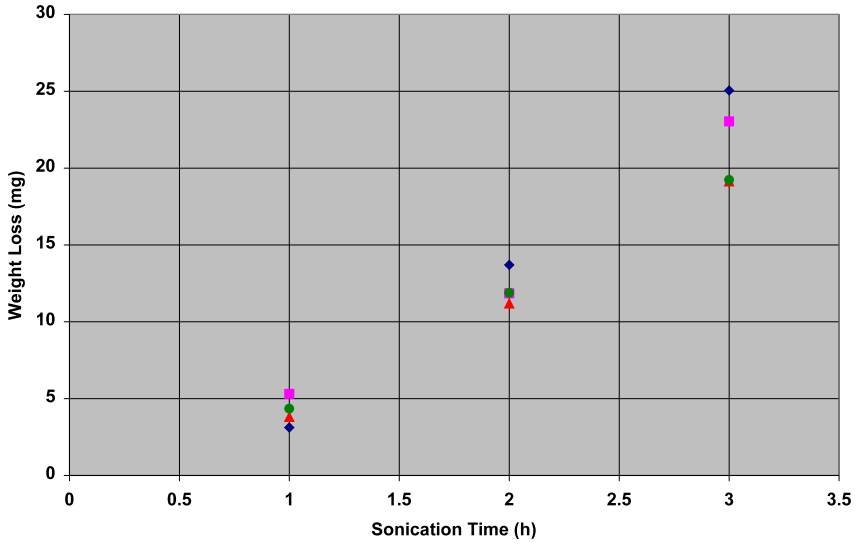

Fig. 2. Specimen weight loss of a function of exposure time for 2 mm specimen depth in pure mercury at 30°C in the glass test vessel (baseline conditions). Note that in some cases, the data points representing the four individual specimens overlap sufficiently to prohibit clear distinction.

Consistent with previous data,[10,11] the weight change as a function of time typically extrapolates to zero weight change at a slightly positive exposure time (rather than zero). This can be generally explained by considering the cavitation-erosion process to require an incubation time in which micro-cracks must be initiated and coalesce/propagate prior to resulting in bulk material loss.[7,16] As a result, it is common for mass loss in the initial exposure period to be somewhat lower than in subsequent exposure periods of similar duration, with an approximately constant mass loss developing after the initial hour or two of exposure.[10,11]

Following sonication, the specimen surface exhibited crudely hemispherical craters that may or may not partially overlap with other nearby craters. Figure 3 is representative of this observation among specimens in this investigation. Examination at higher magnification (series of scanning electron micrographs in Fig. 4) reveals that the cavitation-erosion process apparently involves metal removal in small, progressive stages that has some similarities to micro-cracking/tearing on a small scale. While the spacing of craters was relatively uniform over the specimen surface, it is clear that some feature of the cavitation process tended to focus damage at these individual locations rather than yielding completely uniform removal of material. Young and Johnston[9] noted that cavitation damage in some liquid metals (e.g., Na) tends toward very general attrition while damage in mercury, like that observed here, tends toward formation and deepening of individual craters.

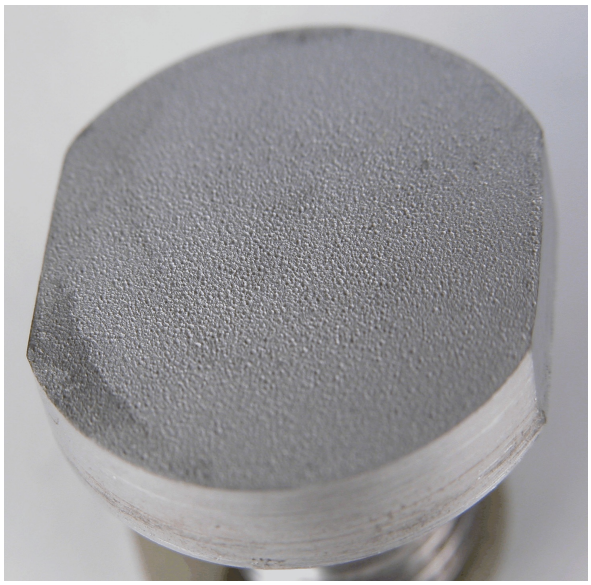

Fig. 3. Vacuum-annealed 316LN stainless steel cavitation specimen following 3 h sonication in pure mercury at room temperature. The actual-size diameter of the specimen is 16 mm.

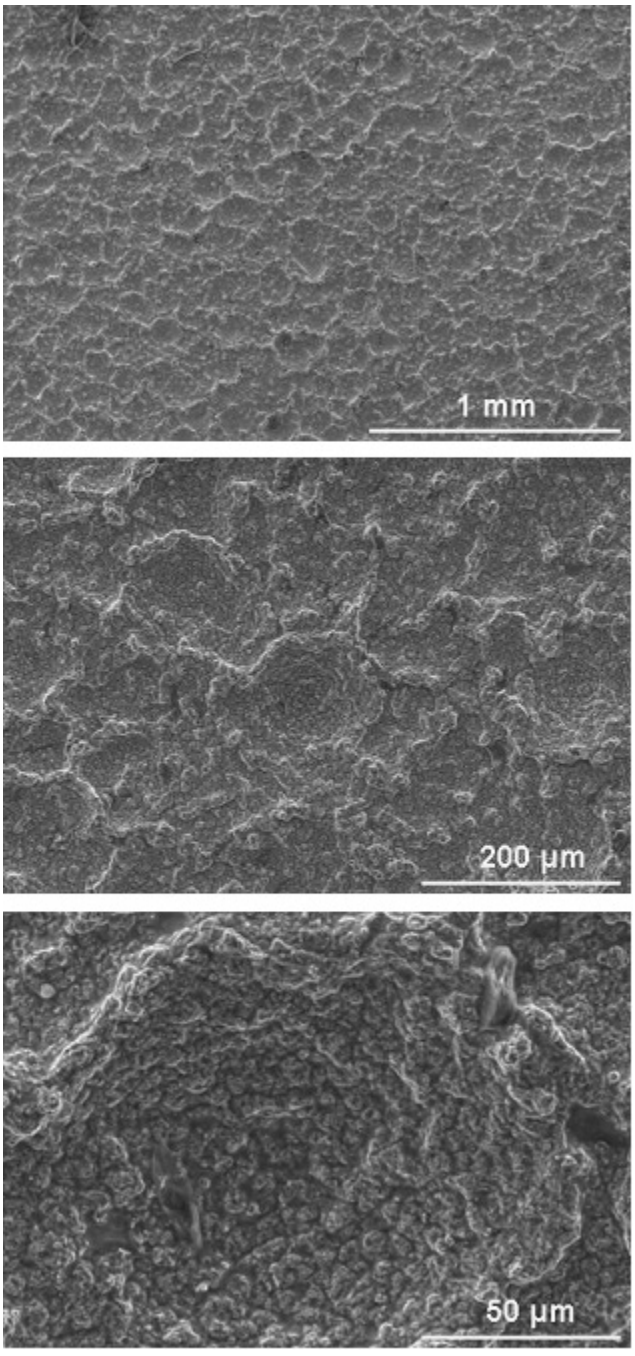

Fig. 4. Backscattered electron images of the cavitation-erosion damage observed on annealed 316LN specimens following 3 h of sonication in pure mercury at room temperature. Magnification increases in sequence from the top photo to the bottom photo.

The surface profile measurement is essentially an assessment of the average depth (rim to bottom) of the craters across the specimen surface. Neither the diameter of the craters, their position relative to the original specimen surface, nor the fraction of the surface represented by craters, is assessed by the profile measurement. These factors would tend to present themselves in the mass loss measurement. Increased profile depth generally correlates with increased mass loss for these specimens, but there are minor exceptions among closely spaced data points. As a rule, the surfaces of the specimens tested in baseline conditions were remarkably uniform in that the average profile was very consistent across the entire specimen. However, as exposure time increased, each specimen exposed in the baseline conditions developed some (as few as two, as many as six) scattered "pits" on the surface. This pattern has been observed previously[9–11] and, like the previous experience, the "pits" observed here were invariably small (surface area less than 0.5 mm^2) and round but relatively deep (commonly 1.5–3 times the nominal profile height) following 3 h of sonication. The mechanism of formation of these "pits" is not clear, but it is possible that they are related to the presence of inclusions intersecting the exposed surface, or rare/random mercury wave conditions in which constructive interference generates an unusually large cavitation pulse.

The average surface profile as a function of exposure time is given for the baseline conditions in Fig. 5. Notice that the intercept of the profile trend line is greater than zero. Interpretation is hampered by a lack of very short-time exposure data, but the positive intercept implies localized erosion damage of susceptible areas occurs very quickly. This explanation is consistent with previous results[4–6, 16] indicating the development of surface roughness and shallow pits after a very few pressure cycles. The positive intercept could also imply that once macroscopic damage is initiated, there is a minimum size/depth for damage that is related to some aspect of the test material (e.g., grain size or sub-cell size) and/or a property of the cavitating fluid.

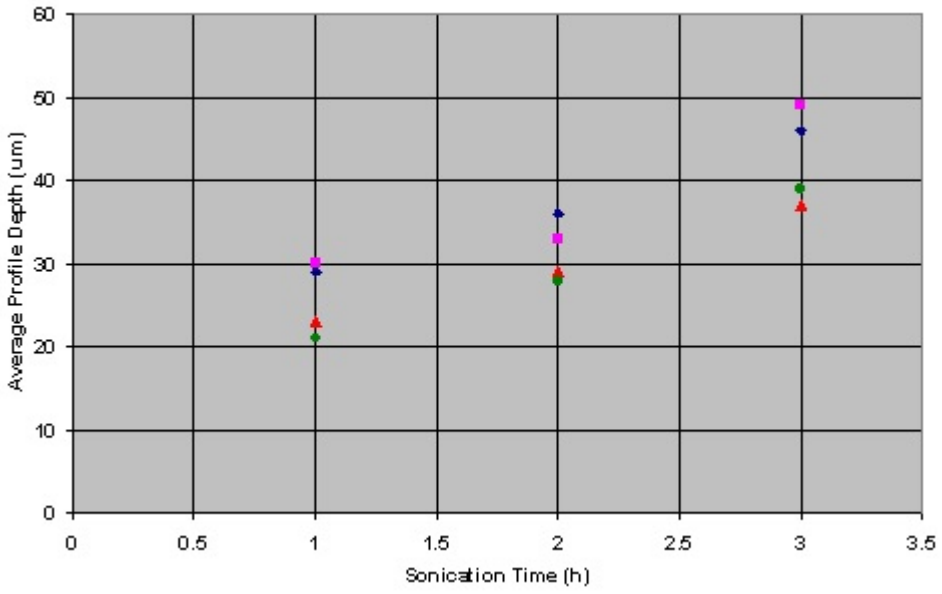

Fig. 5. Surface profile development as a function of exposure time for the baseline test conditions.

Previous cavitation testing at ORNL[10–11] utilized a significantly larger volume of mercury (~750 ml vs. 30 ml) and much greater specimen immersion depth (25 mm vs. 2 mm) than used in the present case. Figure 6 compares the present weight loss data as a function of exposure time for the baseline conditions (immersed 2 mm in a small glass vessel) with other tests in pure mercury at 25–30°C:

(a) 100 ml mercury in a small glass vessel, immersed 25 mm; and

(b) 750 ml mercury in a large stainless steel vessel, immersed 25 mm.

Figure 6 reveals that immersion depth in the glass test container is not a significant variable, with the results falling along the top end of the baseline data scatter band. The results described in terms of average profile depth are analogous. However, 50–60% greater mass loss (and correspondingly greater depth of attack) was observed for testing at 25 mm immersion in the large stainless steel container. While the latter results do not influence the comparison tests reported here, they do indicate that test configuration is a potentially significant variable for cavitation testing of this type and that only results from like configurations should be compared.

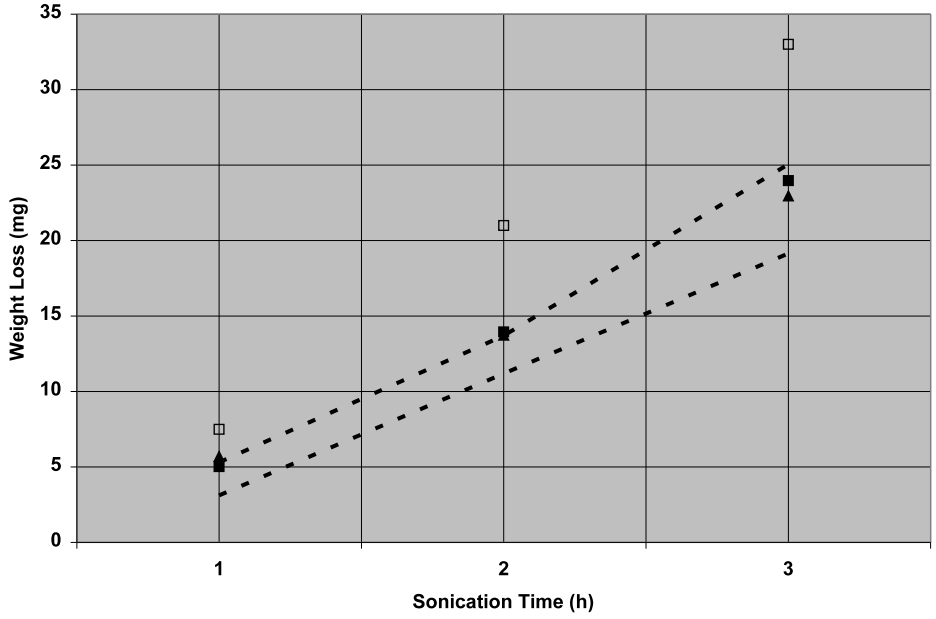

Fig. 6. Weight loss as a function of exposure time for baseline conditions (baseline results from Fig. 2 for 2 mm immersion in 30 ml mercury bounded by the dashed lines) compared with 25 mm immersion in 100 ml mercury within a small glass vessel (solid data points) and 25 mm immersion in 750 ml mercury within a large stainless steel vessel (open data points).

Another observation was that in the cavitation tests in which the specimens were immersed only 2mm – in pure mercury as well as the alloyed mercury described subsequently – the surface of the mercury bath roiled violently and bubbles resulting from the violent agitation of the mercury could periodically be seen escaping from the test surface. For specimens immersed 25 mm, the surface of the mercury bath was calm with no motion readily detectable visually. Apparently, immersion depth influences the macroscopic manifestation of cavitation via increasing the time and/or linear distance for dispersion of the ultrasonic energy introduced into the mercury, and the increased hydrostatic pressure at greater immersion depth may also play a role.

Independent of vessel type or specimen immersion depth, the post-test appearance of the pure mercury in all cases included the slow accumulation of a dark gray/green or black scum floating on the top that appeared to be test debris. Such material accumulates on the mercury surface independent of the test material (observed for sonication of 316LN as well as other materials),[10–11] and is easily skimmed off the surface with cheesecloth. This material has not been analytically identified, but it seems likely that it represents the interaction of mercury and air on the material removed from

the specimen surface during cavitation-erosion. A similar looking material was found floating on the post test mercury following an extended thermal convection loop test of 316L stainless steel at the outset of the SNS compatibility studies, and the dark green/black scum was found to be primarily amorphous but containing Fe, Cr, Ni (the main components of stainless steel) along with mercury and oxygen.[17]

3.3 Addition of Indium to Mercury

Indium is by far the most soluble element in mercury at near-ambient temperature. A roughly rectangular piece of indium (cut from a cast ingot, sized for the desired mass) was added to the mercury within the glass test vessel under argon cover gas flow. The mercury quickly and completely wetted the indium, and appeared to pull the solid indium down into the liquid via the surface tension associated with complete wetting. Within 2–3 min at room temperature, the mercury had completely dissolved the requisite amounts to generate solutions with 5 wt % and 10 wt % In.

Upon dissolution, the surface luster of the mixture immediately changed from the shiny metallic appearance of the pure mercury to a somewhat more dull/flat silver. In addition, the liquid seemed almost “encased” by a thin, pliable silver/gray scum that moved readily with the liquid. Unlike pure mercury, which can be poured from a glass or plastic bottle with no residual scum, or “tailing”,[12] adhering to the container, the Hg-In mixtures tended to leave a small (compared to the mass of indium added) amount of scum on the bottom/side surfaces of containers when the remainder was poured off. Aggressive stirring prior to pouring seemed to minimize the amount of tailing left behind, but it is impractically difficult to completely eliminate the residual material.

Consistent with the observations of Wilkinson,[12] the alloyed mercury seemed to take on properties similar to a semi-solid or a gel in that the droplets could be elongated slightly upon dispensing from a small diameter nozzle and modest-size droplets could be shaped and segmented easily, which is all but impossible for droplets of pure mercury. Figures 7–8, comparing pure mercury beads with Hg – 10 wt % In beads, are representative of this behavior which was observed for all alloyed mercury in this investigation. The authors suspect that the bead-shaping behavior is not a bulk property of the mercury alloy but is due to the “creaming” reaction that leaves the exposed surface of the mercury alloy bead rich in metallic oxide species, and the relative “stiffness” of this layer promotes the shaping of the droplets. Indirect evidence supporting this concept includes the observation that a syringe inserted into the beads of alloyed mercury and used to remove fluid from the center of the bead leaves a “skin” of silver/gray residual material – not readily pulled into the syringe – that appears not unlike

a deflated balloon. The sub-surface mercury within the bead may indeed have a higher surface tension than pure mercury due to the alloying, as measured by Wilkinson,[12] but surface tension measurements were not carried out in this work. If the surface tension indeed increased as a result of alloying, cavitation-erosion damage might be expected to increase. The reason is that increased surface tension implies an increased driving force to collapse a cavitation bubble, and the increased force might be expected to increase the velocity/force associated with the jetting action of liquid that results.

Fig. 7. Bead of pure mercury on the left assumes and maintains a roughly hemispherical shape despite probing with a plastic rod, while the same size bead of Hg – 10 wt % In on the right has its shape readily manipulated. A plastic rod was dragged through the center of each bead just prior to this photograph. Actual bead size in each case was approximately 15 mm diameter.

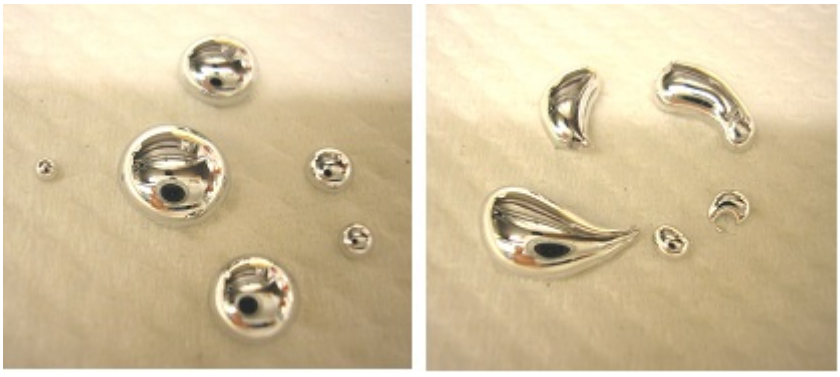

Fig. 8. Small beads of pure mercury on the left resist manipulation and maintain roughly spherical shapes, while the same size beads of Hg – 10 wt % In on the right can be readily shaped. Actual diameter of beads ranged from 2–10 mm.

Weight change as a function of exposure time for the cavitation specimens in mercury with 5 wt % In and 10 wt % In compared to pure mercury is shown in Fig. 9. The data indicate that 5 wt % In generated cavitation-erosion wastage very similar to pure mercury (weight change data falls more-or-less within scatter band for the pure mercury data), while cavitation in 10 wt % In was decidedly more aggressive in terms of weight loss. In particular, note that the apparent incubation time for weight loss seems to be reduced for Hg – 10 wt % In, and at extended exposure times the rate of weight change is also somewhat higher for the Hg – 10 wt % In mixture compared to pure mercury. Consistent with the weight change data, the development of the average profile shown in Fig. 10 also suggests that Hg – 10 wt % In is somewhat more aggressive than pure mercury.

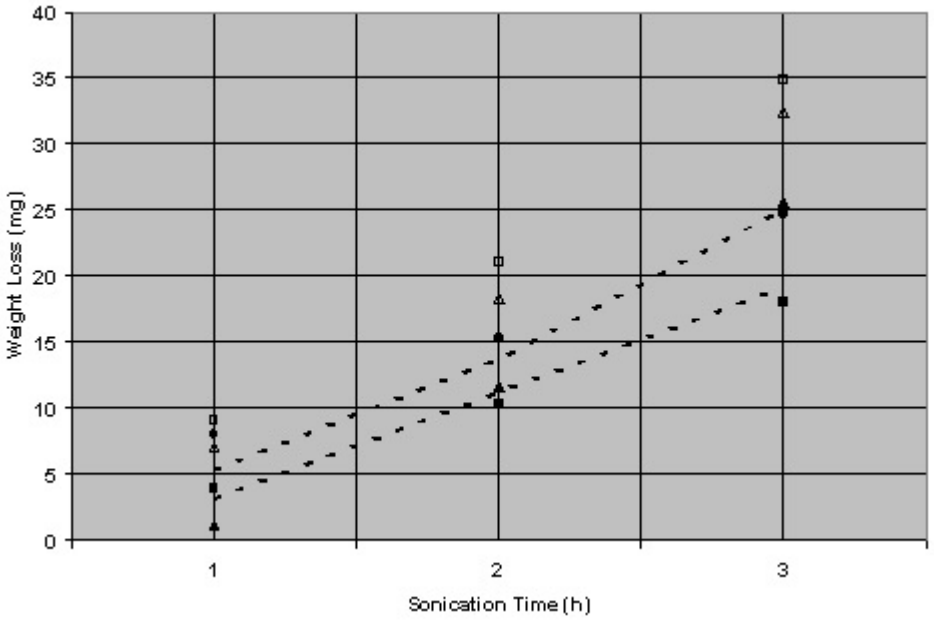

Fig. 9. Weight loss as a function of exposure time for baseline conditions (range of data bounded by dashed lines) compared to Hg – 5 wt % In (solid data points) and Hg – 10 wt % In (open data points).

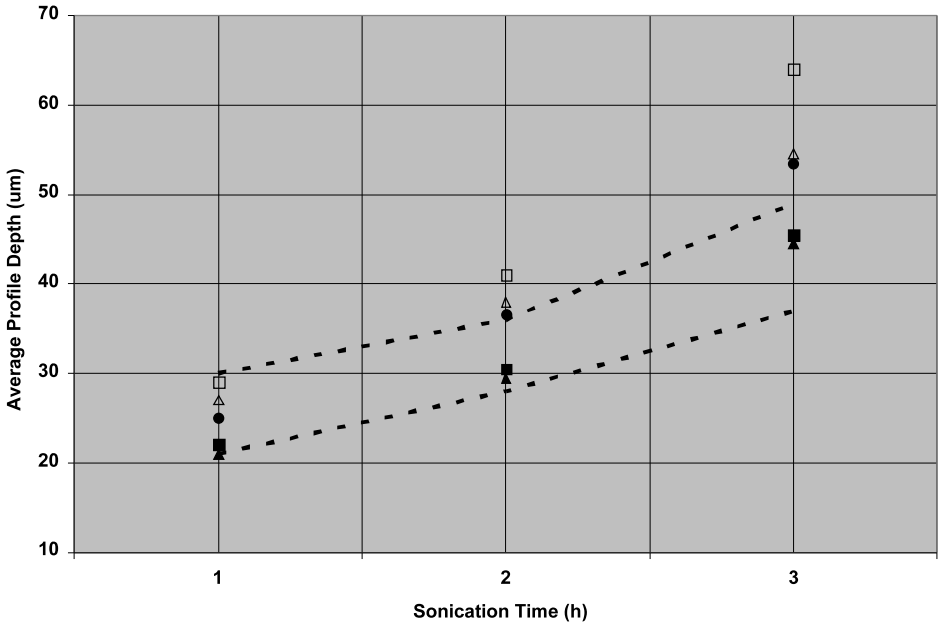

Fig. 10. Average profile depth as a function of exposure time for baseline conditions (range of data bounded by dashed lines) compared to Hg – 5 wt % In (solid data points) and Hg – 10 wt % In (open data points).

While not quantitatively assessed, the addition of indium to the mercury also seemed to make for more tenacious post-test wetting of the specimen. Increased wetting was evidenced by the need for longer post-test cleaning times in the mercury removal step. Representative appearance of the cleaned post-test specimens exposed to Hg + 10 wt % In is given in Fig. 11. Comparison with Fig. 4 reveals that the cavitation-erosion damage process is very similar in pure mercury and alloyed mercury, but clearly the damage profile (depth of the craters) is more defined in the alloyed mercury at the same exposure time. It is also interesting that very few of the “pits” observed on the specimens exposed to pure mercury were observed on specimens exposed to mercury alloyed with indium; of the five total specimens exposed in mixtures of Hg + In, three had no pits and another exhibited only one pit. When the pits were present, however, they were indistinguishable from those observed on other specimens of 316LN exposed in pure mercury.

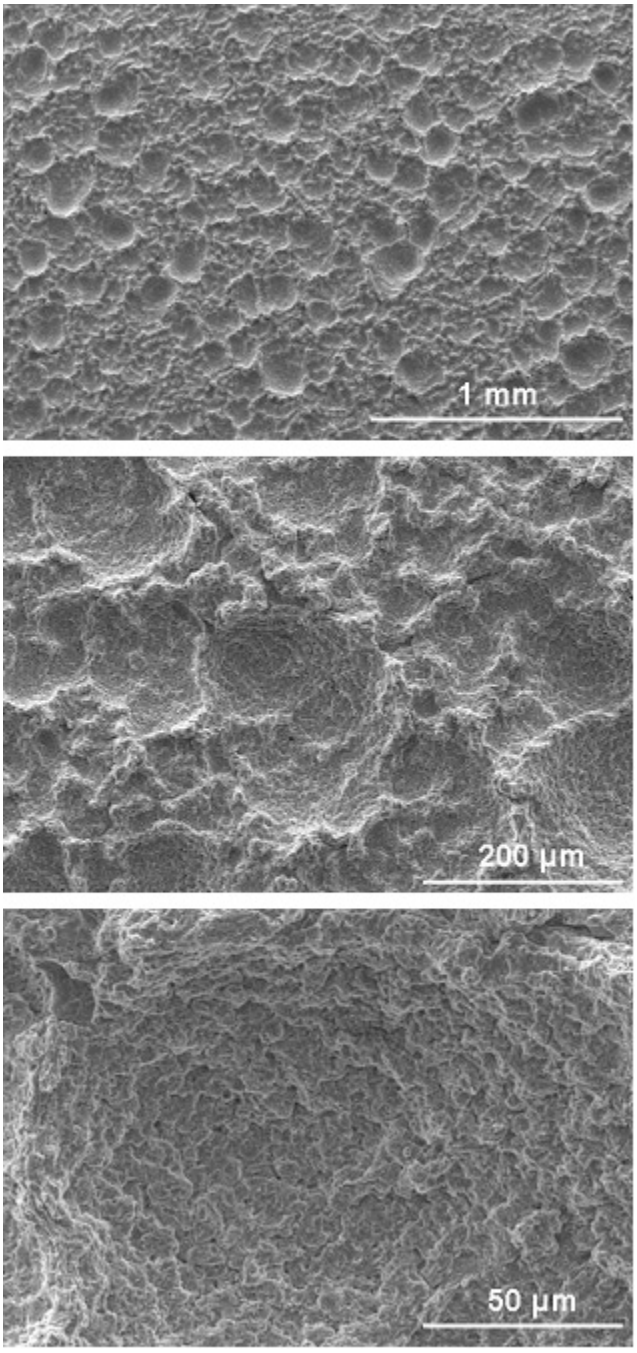

Fig. 11. Backscattered electron images of the cavitation damage observed on annealed 316LN specimens following 3 h sonication in Hg – 10 wt % In at room temperature.

3.4 Additions of Cadmium to Mercury

The room temperature solubility of cadmium in mercury was expected to be near 5 wt %. A roughly cylindrical piece of cadmium (from a larger ingot) sufficient to create a 5 wt % solution was added to mercury at room temperature. The addition was made within the glass test vessel, with the argon cover gas flowing prior to addition of the cadmium. Compared to the behavior with indium, wetting of the cadmium by mercury was somewhat more tentative. Raising the solution temperature from ambient (~22°C) to about 30°C, along with periodic stirring, accelerated wetting/dissolution. After about an hour, only a small piece of the original Cd remained but progress of the dissolution seemed to be seriously slowed or perhaps stalled completely. After about 3 h, when it was clear no further dissolution of Cd would occur, the residual piece of solid Cd was removed from the mercury, cleaned, and weighed. Sufficient Cd had dissolved to create a solution containing approximately 4.4 wt % Cd in mercury. Similar to the situation with In additions, the addition of Cd caused the mercury luster to change from bright/shiny to a dull/flat gray and the liquid to have a modest dull silver scum on the surface. Beads of the Hg-Cd mixture could be manipulated in a similar fashion to that described for the Hg-In mixtures.

As indicated by the data in Figs. 12 and 13, the cavitation-erosion of annealed 316LN in Hg – 4.4 wt % Cd is perhaps slightly more aggressive than in pure mercury. Although the total weight change is similar, the trend is that the rate of weight loss is higher for the Hg-Cd mixture as the exposure time increases, and perhaps a longer test exposure would have discriminated between these test solutions more fully. Interestingly, specimens sonicated in the Hg-Cd solution developed deeper profiles than those sonicated in pure mercury, which is not readily apparent from the weight loss data. Assuming weight loss is related directly to volume of material removed, deeper profile for a similar weight loss suggests that specimens exposed in Hg-Cd have deeper cavitation craters covering less total surface than for specimens exposed in pure mercury.

Post-test wetting of the specimen by the Hg-Cd mixture was very tenacious. Following cleaning, observation of the specimen surfaces revealed only the regular overlapping cratered appearance common to all of these test specimens. After 3 h of exposure, each specimen exhibited 2–3 macroscopically visible pits with depths approximately twice the nominal surface relief, but was otherwise very uniform and essentially identical to the structures indicated in Fig. 11.

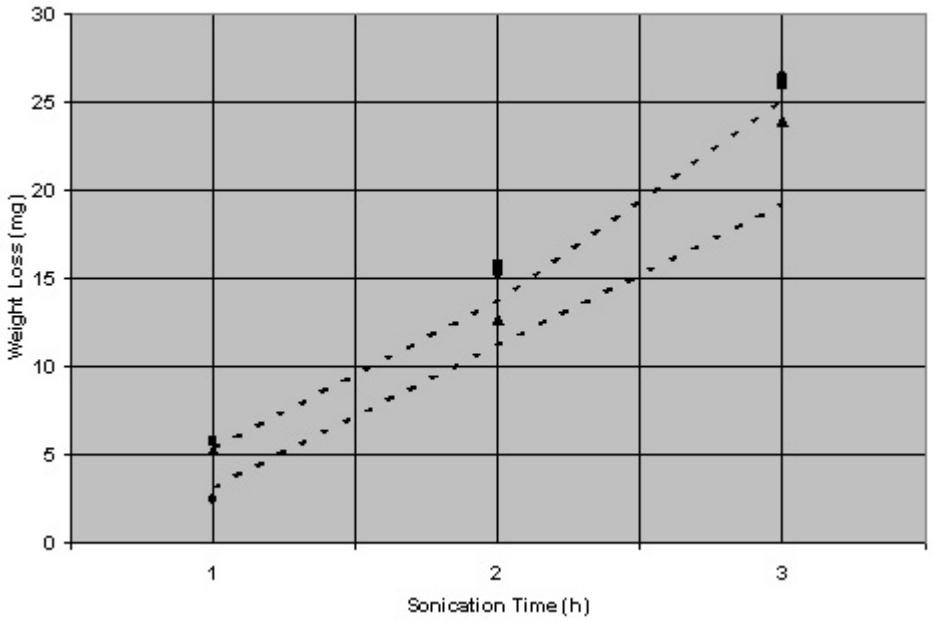

Fig. 12. Weight loss as a function of exposure time for baseline conditions (range of data bounded by dashed lines) compared to Hg – 4.4 wt % Cd (solid data points).

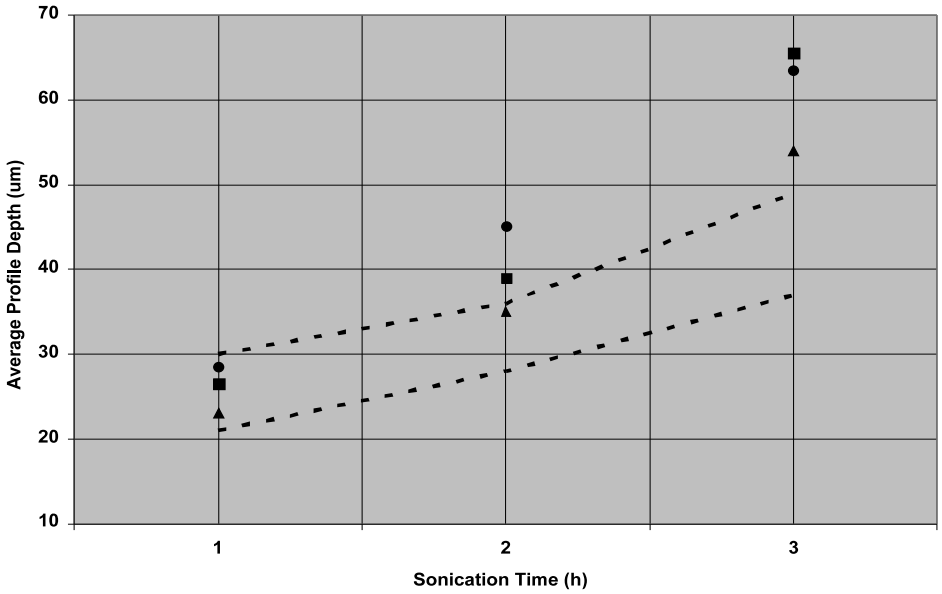

Fig. 13. Surface profile as a function of exposure time for baseline conditions (range of data bounded by dashed lines) compared to Hg – 4.4 wt % Cd (solid data points).

Following the test exposures, the small piece of Cd removed when the dissolution process seemed to have stopped during initial solution preparation was re-added to the solution. No additional dissolution occurred over a period of about 2 h, suggesting the mercury test mixture remained essentially saturated in Cd and therefore that no significant amount of Cd was consumed (either as a scum or via interaction with the test specimen) during the 36 h period required to complete the tests with this mixture.

3.5 Additions of Gallium to Mercury

The room temperature solubility of gallium in mercury was expected to be near 2 wt %. A roughly rectangular piece of ingot gallium sufficient to create a 2 wt % solution was added to mercury at room temperature. The addition was made within the glass test vessel, with the argon flowing prior to addition of the gallium. Wetting of the gallium by mercury was sluggish at room temperature, so the mercury bath temperature was raised to 30°C, which at least partially melted the gallium and noticeably accelerated dissolution/mixing. Upon initial dissolution of this amount of gallium, a modest amount of second phase liquid appeared to form on the surface of the mercury. Droplets of this second phase liquid (likely free gallium) floated and agglomerated much like oil droplets on the surface of water (indicating immiscibility). This second phase has been observed previously[18] and suggests that the solubility of gallium in mercury is actually slightly less than 2 wt % . It was interesting, however, that the second phase liquid was no longer visible after the initial cavitation test in this mixture. It is not clear whether the ultrasonic agitation was effective at stirring and improving intimate mixing or if a small quantity of gallium was consumed in some fashion during the test. For example, gallium could be removed from solution via adhering to specimens following testing or via being splattered high onto the glass container and sticking there.

Figure 14 shows that, in terms of weight loss, cavitation-erosion in 2 wt % Ga is perhaps slightly less aggressive that in pure mercury. However, it is interesting that the surface profile resulting from testing in 2 wt % Ga is somewhat greater than that for testing in pure mercury (see Fig. 15). This observation suggests that the total area of craters at the profile depth is smaller than for specimens tested in pure mercury, but the existing craters tend to be deeper. None of the three specimens exposed to the 2 wt % Ga mixture exhibited pits as previously described, and the cleaned post-test surfaces were essentially identical to the representative photos in Fig. 11.

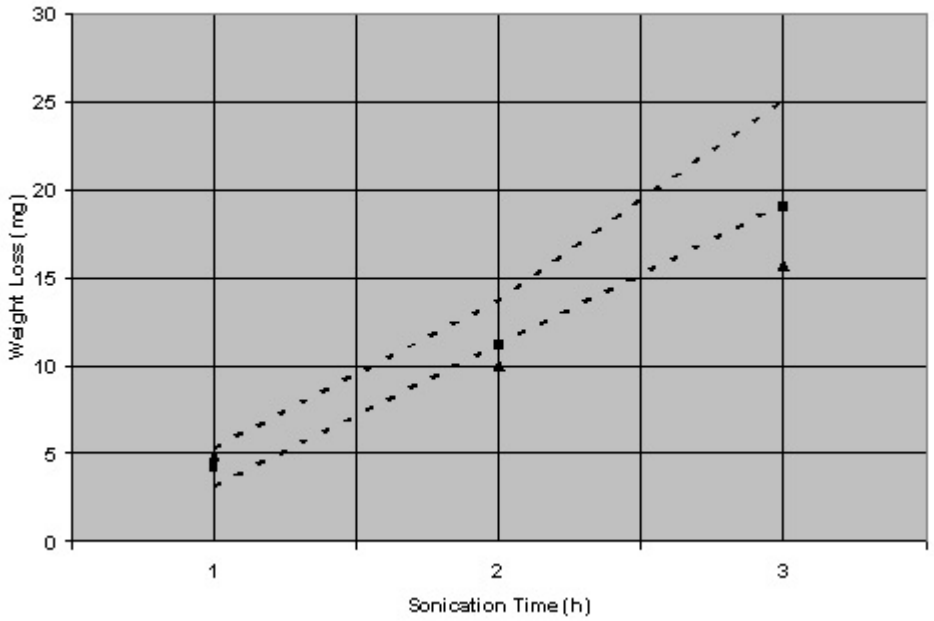

Fig. 14. Weight loss as a function of exposure time for baseline conditions (range of data bounded by dashed lines) compared to Hg – 2 wt % Ga (solid data points).

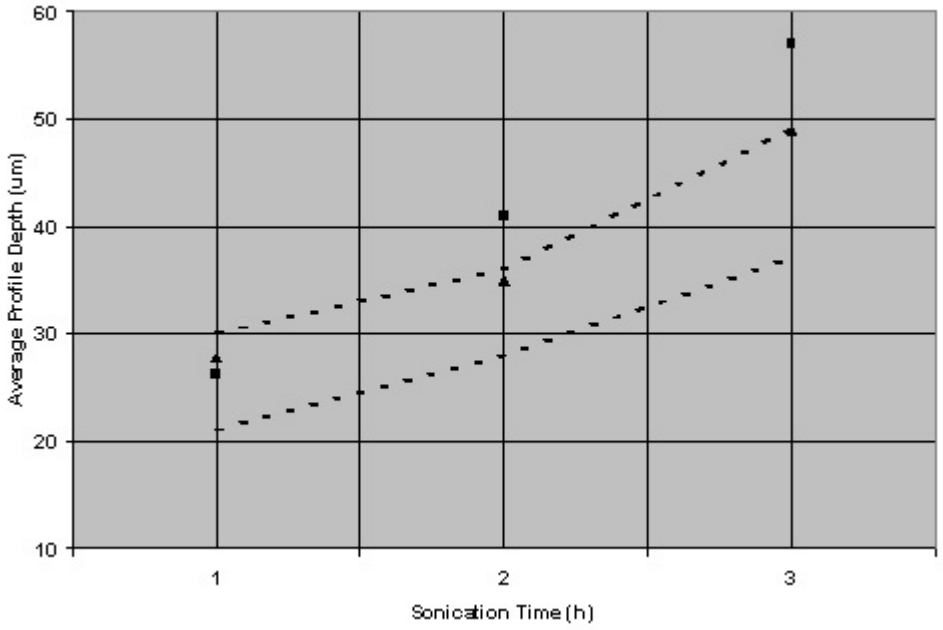

Fig. 15. Surface profile as a function of exposure time for baseline conditions (range of data bounded by dashed lines) compared to Hg – 2 wt % Ga (solid data points).

Post-test observation of the specimens indicated aggressive wetting of the specimen by the 2% Ga mixture. While all of the wetted material seemed relatively shiny silver in appearance, some of the clinging material did not appear to be liquid but behaved more like a solid. In particular, small flecks of material similar to dried paint chips were found on these post test specimens in/on the liquid wetting much of the specimen surface. The identity and/or source of the solid material is not clear at present, but it seems likely that small amounts of gallium may solidify on the test specimens when they are in mercury at less than about 30°C, which is the melting point of gallium.

3.6 Additions of Pb+Sn+Zn to Mercury

Relatively low (~1 wt %) solubility in mercury was expected for each of Pb, Sn, and Zn. An appropriate amount of each solute was added in granular (about 20 mesh) form – simultaneously, under cover of argon – to the host mercury. Dissolution at room temperature was found to be very sluggish, and regular stirring over several hours appeared to have led to dissolution of only about half of the total charge of granules. The zinc appeared to go into solution most slowly, perhaps due to slight oxidation of the granule surfaces. The temperature of the mercury was increased to 30°C and allowed to sit under cover of argon overnight. The following morning, with a little additional stirring over about an hour, very nearly all of the intended solute was dissolved.

As shown in Fig. 16, cavitation-erosion in the 1 wt % Pb – 1 wt % Sn – 1 wt % Zn was somewhat more aggressive than in pure mercury, in absolute magnitude and in rate, as a function of time at 3 h exposure. Consistent with an average weight loss increase of about 50%, the profile depth for the specimens tested in this mixture was also about 50% greater than in pure mercury (see Fig. 17). The increased surface profile on these post-test specimens was remarkably uniform, with only one pit on only one of three specimens with a depth exceeding the nominal profile by a factor of about two. Like the other mixtures, the 1% Pb – 1% Sn – 1% Zn tenaciously wet the specimens but, with a little extra time in the ultrasonic cleaning solution, the liquid metal could be removed from the surfaces. The cleaned post-test surfaces were essentially identical to the representative photos in Fig. 11.

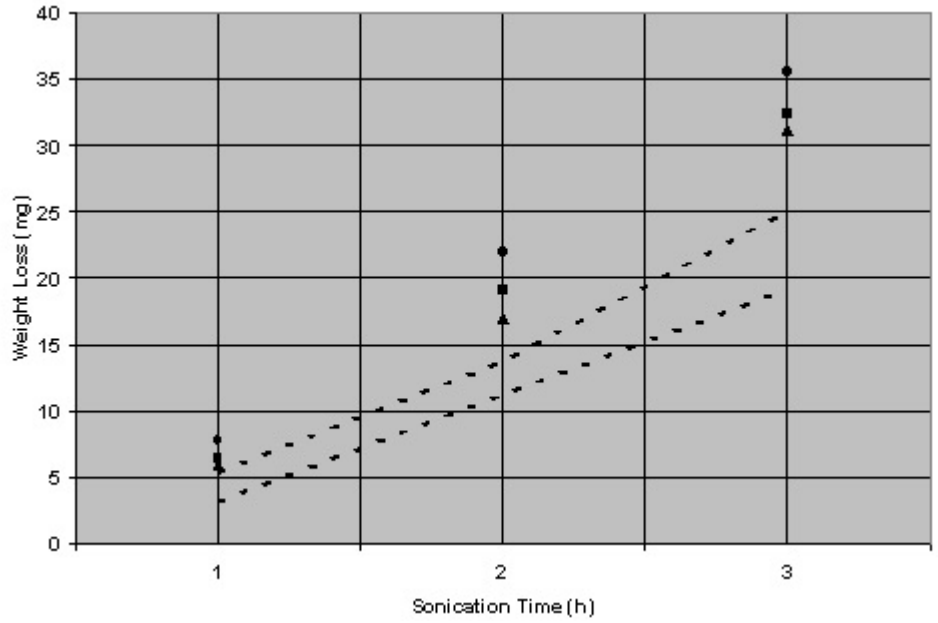

Fig. 16. Weight loss as a function of exposure time for baseline conditions (range of data bounded by dashed lines) compared to Hg – 1 wt % Pb – 1 wt % Sn – 1 wt % Zn (solid data points).

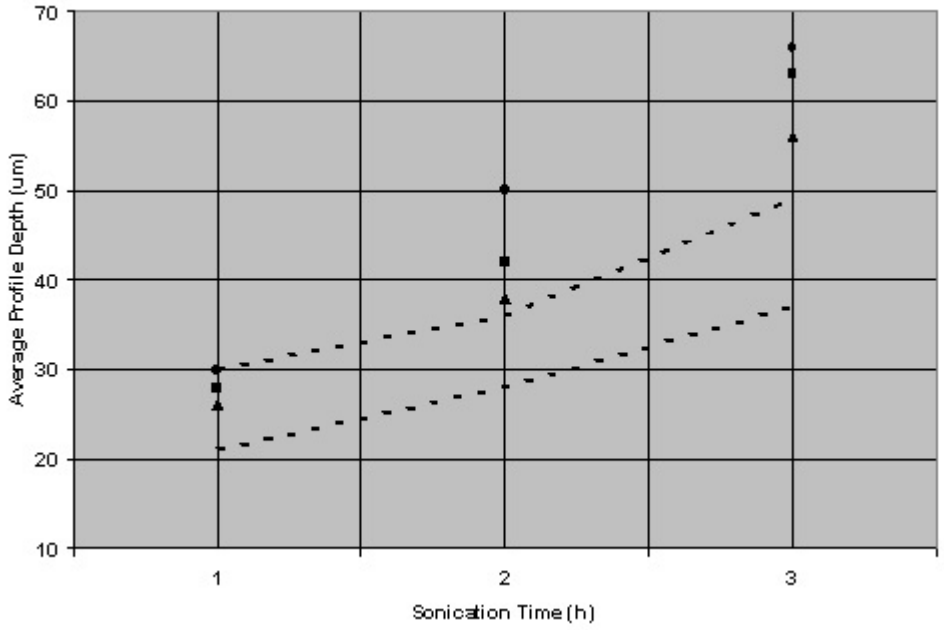

Fig. 17. Surface profile as a function of exposure time for baseline conditions (range of data bounded by dashed lines) compared to Hg – 1 wt % Pb – 1 wt % Sn – 1 wt % Zn (solid data points).

4. CONCLUSIONS

Various metallic solutes were added to mercury in an attempt to change the properties of the resulting liquid metal cavitation medium in a way that might reduce cavitation-erosion damage on annealed 316LN stainless steel. Specimen weight change and profile development as a function of exposure time was compiled for fixed test conditions and compared as a function of the composition of the mercury test medium. Test compositions included pure mercury as well as mercury containing: (a) 5 wt % In, (b) 10 wt % In, (c) 4.4 wt % Cd, (d) 2 wt % Ga, and (e) 1 wt % each of Pb, Sn, and Zn added together.

Compared to pure mercury, mixtures with 10 wt % In and the combination of 1 wt % each of Pb-Sn-Zn significantly increased cavitation-erosion damage as evidenced by significantly greater weight changes and surface profiles – both larger by ~50% – and resulted in a greater rate of change following 3 h of exposure. Solutions including 5 wt % In and 4.4 wt % Cd resulted in weight changes very similar to those observed in pure mercury, but both produced deeper surface profiles, by ~12% and 50%, respectively. Only the solution with 2 wt % Ga exhibited a slightly lower weight loss than that observed in pure mercury after 3 h exposures, but the depth of the surface profile of the specimens so exposed was somewhat greater than for specimens in pure mercury. Based on observation of the cleaned post-test surfaces at a range of magnifications in the scanning electron microscope, the mechanics of cavitation-erosion appear to be the same for pure mercury and alloyed mercury, but perhaps slightly more intense in the latter.

It was observed that alloyed mercury droplets could be shaped and manipulated, suggesting semi-solid properties and perhaps a liquid in which cavitation bubbles would collapse with less intensity than in pure mercury. However, for the conditions and solutes examined here, alloying of mercury did not mitigate cavitation-erosion damage on annealed 316LN stainless steel and, in fact, seems to intensify damage for several mercury alloy compositions. It appears that the semi-solid properties of the mercury are relegated to the near surface regions of the fluid only, caused by a high fraction of oxides in the surface layer, and that the increased surface tension of the bulk (sub-surface) fluid dominates the cavitation-erosion behavior due to increased intensity of bubble collapse. A potential area of interest for future work includes study of the properties of the oxide-rich layer of alloyed mercury exposed to air and whether this semi-solid, wetted onto the test surface of interest, could mitigate cavitation-erosion damage.

5. ACKNOWLEDGMENTS

The Target Development Group of the Spallation Neutron Source (encouraged primarily by B. W. Riemer) provided the funding to support this effort. T. M. Brummett provided the SEM photographs of tested specimens. M. Howell assisted with some of the cavitation tests and photography of the mercury droplets. E. T. Manneschmidt was instrumental in obtaining mercury and small amounts of alloying elements in appropriate form for adding to mercury. J. L. Moser heat treated the test specimens. The Glass Shop at ORNL fabricated the test vessels used for these experiments. F. C. Stooksbury prepared the final manuscript.

6. REFERENCES

1. R. P. Taleyarkhan, F. Moraga, and C. D. West, in: *Proceedings of the 2nd International Topical Meeting on Nuclear Applications of Accelerator Technology (AccApp98)*, Gatlinburg, TN, Sept. 1998, p. 650.

2. F. Moraga and R. P. Taleyarkhan, in: *Proceedings of the 3rd International Topical Meeting on Nuclear Applications of Accelerator Technology (AccApp99)*, Long Beach, CA, Nov. 1999, p. 301.

3. L. K. Mansur and H. Ullmaier, in: *Proceedings of the International Workshop on Spallation Materials Technology,* CONF-9604151, Oak Ridge, TN, April 1996. *Proceedings of the Topical Meeting on Nuclear Applications of Accelerator Technology (AccApp97)*, Albuquerque, NM, Nov. 1997, p. 301.

4. K. Kikuchi, H. Kogawa, M. Futakawa, S. Ishikura, M. Kaminaga, and R. Hino, *J. Nucl. Mater.*, 318 (2003) 84.

5. B. W. Riemer, J. R. Haines, J. D. Hunn, D. C. Lousteau, T. J. McManamy, and C. C. Tsai, *J. Nucl. Mater.*, 318 (2003) 92.

6. J. D. Hunn, B. W. Riemer, and C. C. Tsai, *J. Nucl. Mater.*, 318 (2003) 102.

7. R. Garcia, F. G. Hammitt, and R. E. Nystrom, *Erosion by Cavitation or Impingement*, ASTM STP 408, American Society for Testing and Materials, (1976) 239.

8. M. D. Kass, J. H. Whealton, N. E. Clapp, Jr., J. R. DiStefano, J. H. DeVan, J. R. Haines, M. A. Akerman, and T. A. Gabriel, *Tribol. Lett.*, 5 (1998) 231.

9. S. G. Young and J. R. Johnston, *Erosion by Cavitation or Impingement*, ASTM STP 408, American Society for Testing and Materials, (1967) 186.

10. S. J. Pawel and E. T. Manneschmidt, *J. Nucl. Mater.*, 318 (2003) 122.

11. S. J. Pawel, *J. Nucl. Mater.*, 343 (2005) 101.

12. T. A. Elliott and M. C. Wilkinson, *J. Coll. Int. Sci.*, 40 (1972) 297.

13. T. B. Massalski, ed., *Binary Phase Diagrams,* 2nd Edition, ASM International, 1990.

14. M. C. Wilkinson, *Chem. Rev.*, 72 (1972) 575.

15. *Standard Test Method for Cavitation Erosion Using Vibratory Apparatus*, ASTM G-32-98, American Society for Testing and Materials, Philadelphia, PA, 1998, p. 109.

16. F. G. Hammitt and F. J. Heymann, “Liquid-Erosion Failures,” *Metals Handbook*, 8th Ed., Vol. 10, American Society for Metals, (1975) 160-167.

17. S. J. Pawel, J. R. DiStefano, and E. T. Manneschmidt, *Corrosion of Type 316L Stainless Steel in a Mercury Thermal Convection Loop*, ORNL/TM-13754, Oak Ridge Nat’l. Lab., UT-Battelle, 1999.

18. ORNL Internal Correspondence, S. J. Pawel to T. A. Gabriel, et. al., November 10, 2003.

INTERNAL DISTRIBUTION

1. P. J. Blau
2. J. R. Haines
3. D. C. Lousteau
4. L. K. Mansur
5. T. J. McManamy
6-8. S. J. Pawel
9. B. W. Riemer
10. P. F. Tortorelli
11. M. W. Wendel
12. D. F. Wilson
13. S. J. Zinkle
14. Central Research Library
15. ORNL Laboratory Records–RC